Journal of Pharmaceutical Analysis 12 (2022) 583–589

Contents lists available at ScienceDirect

Journal of Pharmaceutical Analysis

journal homepage: www.elsevier.com/locate/jpa

Original article

Covalent organic nanospheres as a fiber coating for solid-phase microextraction of genotoxic impurities followed by analysis using GC-MS

Yanfang Zhao [a, b], Jingkun Li [b], Hanyi Xie [a, b], Huijuan Li [a, b], Xiangfeng Chen [a, b, *]

[a] School of Pharmaceutical Sciences, Qilu University of Technology (Shandong Academy of Sciences), Jinan, 250014, China
[b] Shandong Analysis and Test Center, Qilu University of Technology (Shandong Academy of Sciences), Jinan, 250014, China

ARTICLE INFO

Article history:
Received 9 March 2021
Received in revised form
4 December 2021
Accepted 5 December 2021
Available online 8 December 2021

Keywords:
Covalent organic nanospheres
Solid-phase microextraction
Genotoxic impurities
Gas chromatography-mass spectrometry

ABSTRACT

Covalent organic nanospheres (CONs) were explored as a fiber coating for solid-phase microextraction of genotoxic impurities (GTIs) from active ingredients (AIs). CONs were synthesized by an easy solution-phase procedure at 25 °C. The obtained nanospheres exhibited a high specific surface area, good thermostability, high acid and alkali resistance, and favorable crystallinity and porosity. Two types of GTIs, alkyl halides (1-iodooctane, 1-chlorobenzene, 1-bromododecane, 1,2-dichlorobenzene, 1-bromooctane, 1-chlorohexane, and 1,8-dibromooctane) and sulfonate esters (methyl *p*-toluenesulfonate and ethyl *p*-toluenesulfonate), were chosen as target molecules for assessing the performance of the coating. The prepared coating achieved high enhancement factors (5097–9799) for the selected GTIs. The strong affinity between CONs and GTIs was tentatively attributed to π–π and hydrophobicity interactions, large surface area of the CONs, and size-matching of the materials. Combined with gas chromatography-mass spectrometry (GC-MS), the established analytical method detected the GTIs in capecitabine and imatinib mesylate samples over a wide linear range (0.2–200 ng/g) with a low detection limit (0.04–2.0 ng/g), satisfactory recovery (80.03%–109.5%), and high repeatability (6.20%–14.8%) and reproducibility (6.20%–14.1%). Therefore, the CON-coated fibers are promising alternatives for the sensitive detection of GTIs in AI samples.

1. Introduction

Genotoxic impurities (GTIs) are found in active ingredients (AIs) synthesized by various pharmaceutical processes [1,2]. As these impurities can directly damage DNA [3], the guidelines of many pharmaceutical regulatory agencies such as the U.S. Food and Drug Administration, the European Medicines Agency, and the United States Pharmacopeia have recently limited the levels of GTIs in medicines. These guidelines define a human daily intake level that exerts no adverse effects. The maximum acceptable intake, beyond which toxicological effects may arise, is 1.5 μg/day [4,5]. Under these stringent guidelines and control strategies, pharmaceutical companies and regulatory communities are compelled to develop and identify sensitive analytical methods for controlling and monitoring trace-level impurities in AIs. Analytical methodologies for GTI detection must be highly selective because GTI structures are both complex and diverse. Thus so far, GTIs have been mainly analyzed using gas chromatography-mass spectrometry (GC-MS) [6] and liquid chromatography-mass spectrometry (LC-MS) [7]. GC-MS is an especially efficient analytical platform with excellent separation capability and high robustness. Chen et al. [8] reported a GC-MS method that detects high-boiling-point epoxide GTIs in drug substances. Liu et al. [9] determined trace levels of mutagenic alkyl toluenesulfonate impurities for controlling the quality safety of AIs. Scherer et al. [10] reported a GC-MS strategy with a low detection limit for analyzing leachable compounds.

Peer review under responsibility of Xi'an Jiaotong University.
* Corresponding author. School of Pharmaceutical Sciences, Qilu University of Technology (Shandong Academy of Sciences), Jinan, 250014, China.
E-mail address: qlgdchenxf@126.com (X. Chen).

https://doi.org/10.1016/j.jpha.2021.12.002

The complexity of AI composition and interference from matrix effects necessitates an advanced pretreatment approach. To meet the stringent requirements of GTI quantification in diverse pharmaceutical matrices, researchers have adopted traditional extraction and microextraction strategies. The traditional pretreatment techniques (direct dissolution and injection) generally lack the required sensitivity for analyzing certain GTIs. Among the microextraction techniques, solid-phase microextraction (SPME) is recognized for its high analytical sensitivity and efficiency [11–13]. Compared with traditional extraction, SPME is merited by higher thermal desorption [14,15], lower solvent consumption, less waste generation, excellent sensitivity, and a simple operating procedure [16,17].

Coating materials play an important role in SPME performance evaluations. SPME coatings have been fabricated from a variety of nanomaterials, including graphitic carbon nitrides [18], ionic liquids [19], metal-organic frameworks [20], molecularly imprinted polymers [21], and covalent organic frameworks (COFs) [22]. A novel type of nanospherical material known as covalent organic nanosphere (CON) has emerged as an effective separation material in high-resolution GC. CONs can be prepared via a facile and rapid process, whereas COFs usually need a long preparation time, sealed high-temperature resistant tube, and protective gas [23]. In addition, CONs provide coincident morphology, outstanding dispersibility, and good chemical, thermal, and organic solvent stabilities [24]. Considering the superior performance, abundant π elements, and hydrophobic characteristics of CONs, we hypothesized that CON-based adsorption substrates can improve the enrichment of compounds for low-concentration detection in AI analysis.

Herein, microporous CONs were fabricated by a Schiff base reaction at room temperature and applied as a novel SPME coating for GTI extraction. The AI preparation procedures are extendible to genotoxic reagents, organic solvents, and catalysts. The performance of the CON coating was tested on two types of GTIs-alkyl halides (1-iodooctane, 1-chlorobenzene, 1-bromododecane, 1,2-dichlorobenzene, 1-bromooctane, 1-chlorohexane, and 1,8-dibromooctane) and sulfonate esters (methyl *p*-toluenesulfonate and ethyl *p*-toluenesulfonate). The compounds in the capecitabine and imatinib mesylate samples were analyzed via GC-MS operated in the selected ion monitoring (SIM) mode. The possible adsorption mechanism was also investigated. In pharmaceutical laboratories, the GC-MS instrumentation is commonly used for quality-control testing and the investigation and detection of alkyl halides and sulfonate esters formed during capecitabine and imatinib mesylate production.

2. Experimental

2.1. Chemicals and reagents

The reagents and chemicals were of analytical grade or better. The standard solutions used in the experiment were prepared with methanol. Tris(4-aminophenyl) amine (TAPA, 96%) and tris(4-formylphenyl) amine (TFPA, 98%) were purchased from Tokyo Chemical Industry Co., Ltd. (Tokyo, Japan). Glacial acetic acid (99.5%), *N*,*N*-dimethylformamide (DMF, 99.8%), ethanol (99.5%), and hydrofluoric acid (40%) were obtained from Shanghai Macklin Biochemical Co., Ltd. (Macklin, Shanghai, China). Chromatographic pure acetone, methanol, *n*-hexane, and dichloromethane were purchased from Tenia Company, Inc. (Phoenix, AZ, USA). Hydrochloric acid and sodium hydroxide were supplied by Kemal Chemical Reagent Co., Ltd. (Tianjin, China). 1-Iodooctane (98%), 1-chlorobenzene (>99%), 1-bromododecane (97%), 1,2-dichlorobenzene (99%), 1-bromooctane (99%), 1-chlorohexane (99%), and 1,8-dibromooctane (98%) were purchased from Sigma-Aldrich Chemical Corp. (Milwaukee, WI, USA). Methyl *p*-toluenesulfonate (98%) and ethyl *p*-toluenesulfonate (98%) were purchased from Tokyo Chemical Industry Co., Ltd. (Tokyo, Japan). Silicone sealant was bought from ABRO Industries Inc. (Berlin, Germany).

2.2. Instrumentation

The morphology of the solvent was observed by scanning electron microscopy (SEM) on a SWPRA™ 55 scanning electron microscope manufactured by Carl Zeiss Micro Imaging Co., Ltd. (Jena, Germany). Transmission electron microscopy (TEM) was conducted on a JEM-2100 transmission electron microscope manufactured by JEOL Co., Ltd. (Tokyo, Japan). Thermogravimetric analysis (TGA) of the CONs was performed on an STA 449F3 Simultaneous Thermal Analyzer (Netsch Co., Ltd., Selb, Germany) between 60 and 800 °C under an N_2 flow rate of 10 mL/min. Powder X-ray diffraction (PXRD) data were recorded using a Bruker Smart Apex charged coupled device-based diffractometer (Bruker Co., Ltd., Karlsruhe, Germany). The N_2 adsorption-desorption isotherms (77 K) of the CONs were measured using a porosimeter (SAP 2460; Micromeritics Instruments Corporation, Norcross, GA, USA). Fourier transform-infrared (FTIR) spectroscopy was performed using a Nicolet iS5 Spectrometer obtained from Thermo Fisher Scientific Inc. (Waltham, MA, USA). Centrifugation was operated with a Multifuge X1R centrifuge obtained from Thermo Fisher Scientific Inc.

2.3. GC-MS parameters

All GTIs were analyzed using a single quadrupole GCMS-QP2020 NX gas chromatograph-mass spectrometer (Shimadzu, Tokyo, Japan) equipped with a split/splitless injection port and an electron ionization chamber. The carrier gas was helium (>99.999%) with the flow rate adjusted to 1.0 mL/min. The GTIs were chromatographically separated on a fused silica DB-5MS capillary column (length: 30 m; inner diameter: 0.25 μm; film thickness: 0.25 μm). The oven temperature was first maintained at 40 °C for 1 min and then increased at 10 °C/min to 280 °C, where it was maintained for 1 min. The source temperature was maintained at 230 °C and the front injector temperature was adjusted to 280 °C. The analytes were quantified in SIM mode. The peaks of each compound were identified by their retention time and the ratios of quantifier and qualifier ions (Table 1). The Henry's law constants of the analytes are presented in Table S1 [25–29].

2.4. Fabrication of CON-coated SPME fiber

The CONs were prepared via a known Schiff base reaction [30] with minor modifications. C_{3v}-symmetric TFPA (116.1 mg) and TAPA (130.6 mg) were mixed and dispersed in 2 mL of DMF. Subsequently, 25 mL of methanol was added to the mixed solution and the mixture was stirred for 10 min at 25 °C. After injecting 10 μL of acetic acid, the mixture was left to further react for 30 min at room temperature. The resultant deep yellow solid was harvested by centrifugation at 7104 *g* for 10 min, washed three times with ethanol (20 mL/wash), and dried in a vacuum overnight at 25 °C.

The coating procedure (Fig. S1) was a slightly modified version of our previous procedure [31]. Before fabricating the CON-coated SPME fiber, stainless steel wires were ultrasonically cleaned in acetone and methanol and then etched in hydrofluoric acid for 40 min. All of these procedures were conducted at room temperature. The etched stainless steel wires were then rinsed with deionized water and the CONs were immobilized on its surface using the silicone sealant coating method [32]. In this process, the prepared stainless steel support was dipped in silicone sealant and then immersed for 10 min in 1 mL of an ethanol suspension containing 100 mg of CONs. Afterward, the fabricated CON-coated SPME fiber

Table 1
Quantification and qualification of the ions of genotoxic impurities (GTIs) by GC-MS (selected ion monitoring mode).

Analyte	Retention time (min)	Quantification ions [a] (*m/z*)	Qualification ions [b] (*m/z*)	Enrichment factors
Chlorobenzene	4.38	91	55 and 93	6102 ± 179
1-chlorohexane	4.56	91	41 and 55	5648 ± 178
1,2-dichlorobenzene	7.68	146	75 and 111	8076 ± 573
1-bromooctane	9.45	135	57 and 137	6194 ± 186
1-iodooctane	10.89	57	43 and 71	6587 ± 149
1,8-dibromooctane	15.04	69	111 and 135	5097 ± 122
1-bromododecane	15.14	135	57 and 137	5115 ± 163
Methyl *p*-toluenesulfonate	14.24	91	155 and 186	9590 ± 328
Ethyl *p*-toluenesulfonate	17.70	91	155 and 200	9799 ± 750

[a] When mass spectrum conditions are optimized, the ions with the highest sensitivity and no interference are selected as the quantification ions.
[b] When mass spectrum conditions are optimized, the two ions with the highest sensitivity comprise qualification ions.

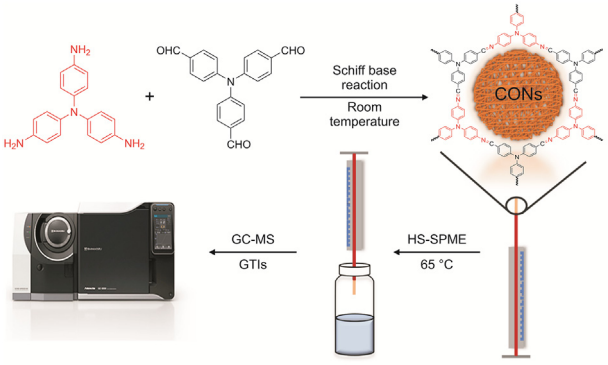

Scheme 1. Preparation of CON-coated fiber and its application. CONs: covalent organic nanospheres; GC-MS: gas chromatography-mass spectrometry; GTIs: genotoxic impurities; HS: headspace; SPME: solid-phase microextraction.

was placed in a GC injector at 280 °C for 3 h. The preparation and application of the CON-coated fiber are illustrated in Scheme 1.

2.5. Sample pretreatment

Standard stock solutions of 1-iodooctane, 1-chlorobenzene, 1-bromododecane, 1,2-dichlorobenzene, 1-bromooctane, 1-chlorohexane, 1,8-dibromooctane, methyl methane sulfonate, and ethyl methane sulfonate were prepared by accurately dissolving weighed reference standards in methanol. The solutions were stored at −20 °C until use. Capecitabine and imatinib mesylate were crushed into fine powders and stored at 4 °C. A series of standard working solutions (0.2–100 ng/g) of GTIs were then prepared in water containing blank sample matrices. For real sample analysis, the actual samples were spiked with GTI standard solution.

2.6. SPME procedure

A mixture of deionized water (10 mL), analyte-free AI sample (50 mg), and a salting-out agent (NaCl) was placed in a 20-mL borosilicate headspace vial. The mixture in the vial was homogenized using a Teflon-coated magnetic stirrer bar. After stirring, the vial was sealed with silicon-polytetrafluoroethylene septa and preserved as the blank control group. The pH and ionic strength of the mixture solution were 7 and 7%, respectively. The stirring rate was set to 800 r/min. All experiments were performed in headspace SPME mode. Initially, the vials were placed in a constant-temperature magnetic stirrer (Xi'an Yima Optoelec Co., Ltd., Xi'an, China) and allowed to equilibrate at the targeted temperature for 10 min. The analytes were exposed to the CON-coated fiber for 35 min. The fiber was subsequently placed in the vials to adsorb the evaporated GTI molecules and then immediately placed in the GC injector at a desorption temperature of 280 °C, where the GTIs were allowed to desorb for 5 min to prevent carry-over effects.

3. Results and discussion

3.1. Characterization of the adsorbent

As shown in the SEM image (Fig. 1A), the CONs were uniform spheres with a diameter of approximately 400 nm. The size of the CONs determined from the TEM image (Fig. 1B) agreed with that obtained from the SEM image. In the FTIR spectrum (Fig. 1C), the C=O bond at 1695 cm^{-1} was attributed to TFPA and the characteristic bands at 3406 and 3337 cm^{-1} were attributed to the N–H bonds of TAPA. The characteristic bands of C=C at 1588 cm^{-1} and C=O at 1695 cm^{-1} corresponded to free TAPA and TFPA, respectively. Results suggested the presence of π–π interactions between the CONs and analytes during the extraction process. The bonds at 1619 and 1269 cm^{-1} were assigned to C=N and C–N bonds, respectively. The specific surface area (SSA) of the synthesized CONs, determined from the nitrogen adsorption-desorption isotherm, was 203.5 m^2/g, and the pore size was 2.3 nm (Fig. 1D). The high surface area and microporosity favored the adsorption capacity and compound capture of the samples. Before coating on the stainless steel support, the CON nanoparticles were analyzed by TGA (Fig. 1E). No significant weight loss from the CON nanoparticles appeared until 470 °C. At temperatures above 470 °C, a major degradation stage appeared in the TGA curve, indicating the total collapse of the CON structure and the volatilization of other organic groups. The results confirmed the superior thermal stability of the CONs, which facilitated SPME in the GC injector. The TGA curve of the silicone sealant used to fix the CONs was repeatedly studied at elevated temperatures to check its reconditioning ability. The TGA curve in Fig. S2 confirmed the exceptional thermal stability of the silicone sealant. The structural ordering of the CONs was explored by PXRD. The wide-angle XRD of the product (Fig. 1F) exhibited sharp peaks at $2\theta = 10°$, 23°, and 45°, indicating a well-crystallized structure. To test their chemical stability, the CONs were immersed in HCl (0.1 mol/L) and NaOH (10 mol/L) for 48 h and their PXRD data were recollected. The locations of the peaks remained unchanged, indicating that the CONs were retained after the acid and base treatments. These results indicated the satisfactory chemical stability of the CONs. These favorable features of the resultant CONs will benefit the subsequent detection of analytes in actual complex matrices.

3.2. Optimization of SPME

The optimal stirring rate, pH, ionic strength, extraction and desorption temperatures, and extraction and desorption time were

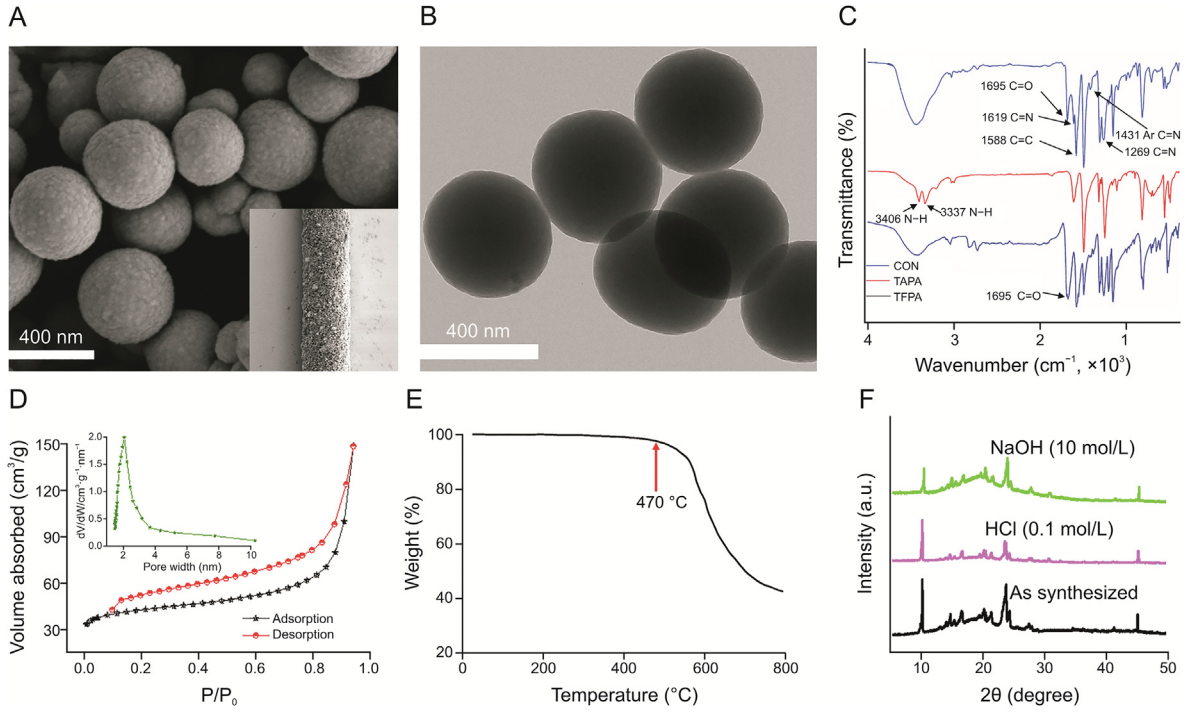

Fig. 1. Characterizations of CONs. (A) Scanning electron microscopy (SEM) and (B) transmission electron microscopy (TEM) of CONs; (C) Fourier transform-infrared (FTIR) spectra of tris(4-aminophenyl) amine, tris(4-formylphenyl) amine, and CONs; (D) specific surface area and pore size (inset: the pore size distribution plot of CONs); (E) thermogravimetric analysis curves of CONs; (F) powder X-ray diffraction (PXRD) pattern of the as-synthesized CONs in HCl (0.1 mol/L) and NaOH (10 mol/L).

explored in the extraction procedures of pharmaceutical samples spiked with GTIs (20 ng/g). The best kinetic and thermodynamic parameters were obtained through the Box-Behnken design (BBD) using the analysis of variance [33]. In a regression analysis, the quadratic model well fitted the BBD setup in the optimization process (confidence level >95%). Panels A–C of Figs. 2 and S3 show the response surfaces obtained by plotting the ionic strength versus extraction temperature, ionic strength versus extraction time, extraction temperature versus extraction time, pH versus stirring rate, and pH versus ionic strength. To explore the potential of the CON-coated fiber, the final parameters were set as follows: extraction temperature 65 °C; extraction time 35 min; ionic strength 7%; pH = 7; and stirring rate 800 r/min. As desorption conditions are significant when assessing the CON-coated fiber, we investigated the effect of desorption temperature on the GTI signal intensity. As illustrated in Fig. 2D, the signal was enhanced by 10% approximately, when the temperature increased from 200 to 280 °C but did not further respond to temperatures above 280 °C. Considering the thermal stability of the fibers, the optimal desorption temperature was determined as 280 °C.

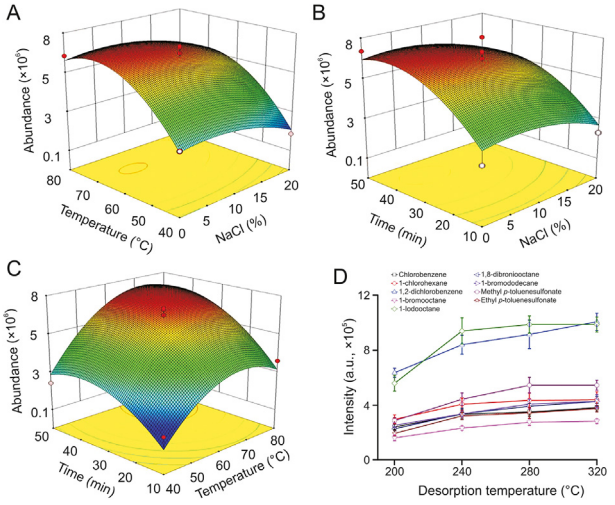

Fig. 2. Optimization of the experimental parameters: (A) ionic strength versus extraction temperature, (B) ionic strength versus extraction time, and (C) extraction time versus extraction temperature (stirring rate: 800 r/min; pH = 7; desorption time: 5 min). (D) Effect of desorption temperature on GTI signal intensity (20 ng/g GTIs).

3.3. Comparison of CON-coated SPME fiber and commercial fibers

To better demonstrate the advantages of CON-coated SPME fiber in the analysis of GTIs from AIs, the performance of the fiber was compared with those of three commercially available fibers, i.e., 100-μm polydimethylsiloxane (PDMS), 65-μm polydimethylsiloxane divinylbenzene (PDMS-DVB), and 85-μm polyacrylate (PA). The enrichment factors (EFs) of all fibers were evaluated with the same working parameters. The CON-coated fiber was 10-μm thick (Fig. S4). In a previous study, the EFs were obtained by calculating the area ratio of the analytes' peaks in the presence and absence of SPME [34]. As described in Fig. 3, the CON-coated fiber demonstrated better extraction performance for alkyl halides, sulfonate esters, and chlorobenzenes than the PA (2.00–9.43 fold), PDMS-DVB (1.88–4.60 fold), and PDMS (2.04–6.30 fold) fibers.

3.4. Possible adsorption mechanisms

The higher EFs of the CON-coated fibers than those of the existing fibers for alkyl halides, sulfonate esters, and chlorobenzenes presumably resulted from the highly conjugated structure of the CON surface. The delocalized π-electrons on the surface enhanced the π–π stacking interactions with the sulfonate esters and chlorobenzenes and increased the hydrophobic effect. The latter feature is important because hydrophobic interactions

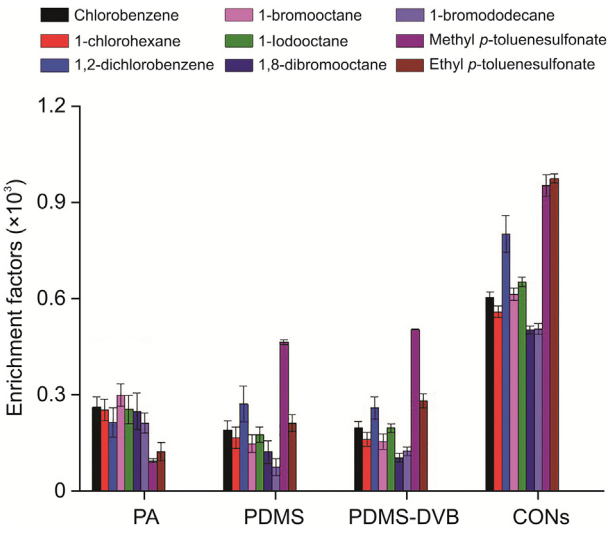

Fig. 3. Comparison of enrichment factors of different fibers (stirring rate: 800 r/min; pH = 7; salt concentration: 7%; extraction temperature: 65 °C; extraction time: 35 min; desorption temperature: 280 °C; time: 5 min). PA: polyacrylate; PDMS: polydimethylsiloxane; PDMS-DVB: polydimethylsiloxane divinylbenzene.

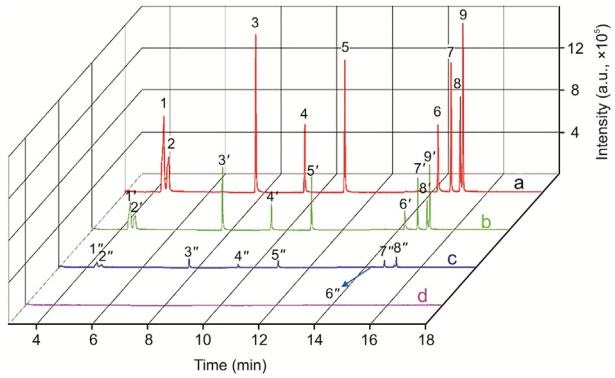

Fig. 4. Sample chromatograms of capecitabine. 1, 1′, and 1″: 1-chlorobenzene; 2, 2′, and 2″: 1-chlorohexane; 3, 3′, and 3″: 1,2-dichlorobenzene; 4, 4′, and 4″: 1-bromooctane; 5, 5′, and 5″: 1-iodooctane; 6, 6′, and 6″: methyl *p*-toluenesulfonate; 7, 7′, and 7″: ethyl *p*-toluenesulfonate; 8, 8′, and 8″: 1,8-dibromooctane; and 9, 9′, and 9″: 1-bromododecane. Sample was spiked at (a) 50, (b) 20, and (c) 10 ng/g; (d) blank. Extraction conditions: salt content: 7%; temperature: 65 °C; time: 35 min. Desorption was performed at 280 °C for 5 min.

mainly govern the interaction between CONs and alkyl halides. Notably, high SSA of an adsorbent facilitates adsorption [35]. Therefore, the high adsorption capacity of CON for GTIs may be attributed to its large SSA. Meanwhile, the size-matching effect along with high thermal stability significantly improved the GTI extraction by CONs. The adsorption between CONs and GTIs could be attributed to the synergistic effect of the hydrophobic interactions, π–π stacking, size-matching effect, and the excellent properties (large SSA and high thermal stability) of the CONs.

3.5. Method validation

The parameters of the methodology are listed in Table 2. The limit of detection (LOD, signal to noise (S/N) = 3) ranged between 0.04 and 2.0 ng/g. The limit of quantification (LOQ, S/N = 10) ranged from 0.15 to 7.0 ng/g. Furthermore, good linear correlation (R^2: 0.9921–0.9998) was obtained over a wide linear range (0.2–200 ng/g). The repeatability and reproducibility of the methodology were assessed by calculating the relative standard deviation (RSD) of multiple spiked blank samples. The repeatability was determined by six replicate tests of a single fiber. The inter-day RSD was from 6.20% to 14.3%, and the intra-day RSD was from 6.30% to 14.8%, respectively. Meanwhile, the reproducibility (ranging from 6.20% to 14.1%) was obtained from parallel investigations on six fibers. The accuracy was obtained from six runs of each compound at three concentrations within the calibration range of the established strategy. The results in Table S2 are the percentage differences from the actual (%DFA) results. The %DFA ranged from −4.68 to 6.66, confirming the satisfactory quantification of GTIs. In addition, after 60 cycles of reuse, the signals of all compounds decreased by only 4.10%–14.5%, confirming the sensitivity and precision of the analytical method.

3.6. Real sample analysis

To demonstrate the applicability of the resulting CON-coated fiber to GTI analysis in actual pharmaceutical samples, the developed method was applied to two AIs, imatinib mesylate and capecitabine. Sample chromatograms of capecitabine were showed in Fig. 4. The recovery (Table 3) was assessed at 10, 20, and 50 ng/g using the equation provided in the Supplementary data. Under the optimal SPME conditions, the recoveries of nine GTIs varied from 80.03% (1,2-dichlorobenzene in imatinib mesylate) to 109.5% (methyl *p*-toluenesulfonate in imatinib mesylate), which are acceptable [36]. Considering the obtained results compared with those of previous reports (Table 4) [6,37–40], our method provided acceptable LODs, a wide linearity range, and satisfactory recovery. In addition, this method exhibited short extraction time and low organic solvent consumption. In future studies, the mechanism of interaction between CONs and the factors influencing their performance should be further investigated, the fiber-to-fiber reproducibility should be improved, and the effectiveness of CONs should be explored in the analyses of other GTIs in complex samples.

Table 2
Method validation summary.

Analyte	Linear range (ng/g)	R^2	LOD (ng/g)	LOQ (ng/g)	Repeatability (RSD%, n=6)		Reproducibility (RSD%, n=6)
					Inter-day	Intra-day	
Chlorobenzene	10–200	0.9921	2.0	7.0	8.90	6.30	6.20
1-chlorohexane	10–200	0.9941	2.0	7.0	14.3	6.70	10.0
1,2-dichlorobenzene	2.0–200	0.9998	0.4	1.5	13.5	14.8	11.6
1-bromooctane	2.0–200	0.9940	0.4	1.5	13.9	8.00	8.90
1-iodooctane	0.2–100	0.9960	0.04	0.15	12.5	7.10	14.1
1,8-dibromooctane	0.2–100	0.9940	0.04	0.15	7.60	11.8	12.9
1-bromododecane	4.0–200	0.9941	1.0	3.5	6.20	10.9	8.30
Methyl *p*-toluenesulfonate	0.2–100	0.9952	0.04	0.15	9.80	9.40	11.0
Ethyl *p*-toluenesulfonate	0.2–100	0.9940	0.04	0.15	11.7	10.3	13.6

LOD: limit of detection; LOQ: limit of quantification; RSD: relative standard deviation.

Table 3
Results of the analysis of nine GTIs in real samples.

Analyte	Imatinib mesylate				Capecitabine			
	Found (ng/g)	Recovery [a] (%)			Found (ng/g)	Recovery [a] (%)		
		10 ng/g	20 ng/g	50 ng/g		10 ng/g	20 ng/g	50 ng/g
Chlorobenzene	ND	91.60 ± 7.95	90.60 ± 5.29	87.44 ± 9.59	ND	88.95 ± 3.35	83.89 ± 8.33	108.3 ± 7.06
1-chlorohexane	ND	83.25 ± 5.34	80.54 ± 3.28	101.1 ± 7.53	ND	86.17 ± 5.78	81.87 ± 5.18	87.25 ± 9.21
1,2-dichlorobenzene	ND	105.3 ± 4.78	80.03 ± 9.11	89.53 ± 11.0	ND	104.2 ± 6.99	94.05 ± 10.3	84.62 ± 6.03
1-bromooctane	ND	83.56 ± 7.61	84.18 ± 6.77	103.9 ± 9.41	ND	100.2 ± 8.7	84.34 ± 6.68	88.27 ± 6.46
1-iodooctane	ND	91.88 ± 4.31	86.67 ± 9.16	106.2 ± 6.44	ND	86.65 ± 3.11	86.25 ± 3.78	82.05 ± 7.16
1,8-dibromooctane	ND	95.06 ± 6.69	87.46 ± 9.35	89.76 ± 6.94	ND	97.94 ± 10.2	82.27 ± 7.44	90.03 ± 9.09
1-bromododecane	ND	89.64 ± 7.43	88.75 ± 6.35	88.36 ± 7.68	ND	89.94 ± 10.89	98.29 ± 9.10	104.0 ± 8.16
Methyl *p*-toluenesulfonate	ND	103.6 ± 9.35	109.5 ± 9.43	87.33 ± 9.69	ND	94.77 ± 11.0	107.6 ± 8.32	90.23 ± 6.68
Ethyl *p*-toluenesulfonate	ND	97.07 ± 5.87	86.63 ± 9.46	91.99 ± 4.63	ND	86.30 ± 5.57	88.25 ± 8.78	103.2 ± 9.59

[a] At different spiked level. ND: not detected.

Table 4
Comparisons of different methods for the solid-phase microextraction (SPME) of GTIs.

Method	Materials	Analytes	Linear range	Correlation coefficient	LOD	Recovery (%)	Refs.
SPME–GC-MS/MS	Ionic liquids	Akyl halides	5–500 μg/L	>0.98	0.3–1.1 μg/L	80.8–117.4	[6]
HS–GC	Ionic liquids	Alkyl/aryl halide	2.5–1.0 × 10^5 ng/g	0.996–0.999	2.5–10 ng/g	75.0–115	[37]
HS–SPME-GC	Polydimethylsiloxane	5 GTIs	0.8–2000 ng/mL	ND	0.08–0.6 ng/mL	ND	[38]
HPLC	Molecularly imprinted polymers	4-dimethylaminopiridine	250–350 μg/mL	ND	ND	98	[39]
LC-MS	Molecularly imprinted polymers	1,3-diisopropylurea	ND	ND	ND	80	[40]
SPME–GC/MS	Covalent organic nanospheres	9 GTIs	0.2–200 ng/g	>0.99	0.04–2.0 ng/g	80.03–109.5	This work

GC: gas chromatography; MS: mass spectrometry; HS: Headspace; HPLC: high-performance liquid chromatography; LC: liquid chromatography; ND: not detected.

4. Conclusion

In conclusion, CONs were successfully implemented as SPME fiber adsorbents that preconcentrate the genotoxic impurities from AIs prior to analysis by GC-MS. The properties of CONs (high SSA, good thermostability, high acid and alkali resistance, favorable crystallinity, and porosity) boosted the enrichment performance of the fiber. Consequently, the fiber exhibited higher EFs (5097–9799) than commercially available PA and PDMS-coated SPME fibers for nine GTIs with different molecular structures. The proposed approach showed high sensitivity with a low detection limit (0.04–2.0 ng/g) and a wide linear range (0.2–200 ng/g). Furthermore, the methodology was successfully applied to GC-MS analysis of real AIs with acceptable recovery (80.03%–109.5%), good repeatability (6.20%–14.8%), and high reproducibility (6.20%–14.1%). The strong adsorption of GTIs on CONs was tentatively attributed to π–π interactions, hydrophobicity, large surface area, and the size-matching effect. The developed method based on the CON-coated fiber and GC-MS accurately analyzed the GTIs from real pharmaceutical samples. Therefore, the CON-coated fibers are potentially applicable to sensitive detection of GTIs in pharmaceutical samples.

CRediT author statement

Yanfang Zhao: Conceptualization, Methodology, Formal analysis, Writing - Original draft preparation; **Jingkun Li:** Conceptualization, Methodology, Formal analysis, Writing - Original draft preparation; **Hanyi Xie:** Investigation, Methodology, Formal analysis; **Huijuan Li:** Methodology, Formal analysis; **Xiangfeng Chen:** Conceptualization, Writing - Original draft preparation, Reviewing and Editing.

Declaration of competing interest

The authors declare that there are no conflicts of interest.

Acknowledgments

This work was supported by the Key Research and Development Program of Shandong Province (Grant No.: 2019GSF111001), the National Natural Science Foundation of China (Grant No.: 21906096), the Youth Science Funds of the Shandong Academy of Sciences (Grant No.: 2019QN009), the Youth Ph.D. Cooperation Funds of Qilu University of Technology (Shandong Academy of Sciences, Grant No.: 2018BSHZ0029), and the Program for Taishan Scholars of Shandong Province (Grant No.: tsqn202103099).

Appendix A. Supplementary data

Supplementary data to this article can be found online at https://doi.org/10.1016/j.jpha.2021.12.002.

References

[1] K. Miyamoto, H. Mizuno, E. Sugiyama, et al., Machine learning guided prediction of liquid chromatography-mass spectrometry ionization efficiency for genotoxic impurities in pharmaceutical products, J. Pharm. Biomed. Anal. 194 (2021), 113781.
[2] N.V.V.S.S. Raman, A.V.S.S. PrasadK, K. Ratnakar Reddy, et al., Determination of genotoxic alkyl methane sulfonates andalkyl paratoluene sulfonates in lamivudine usinghyphenated techniques, J. Pharm. Anal. 2 (2012) 314–318.
[3] P.D. Tzanavaras, S. Themistokleous, C.K. Zacharis, Automated fluorimetric determination of the genotoxic impurity hydrazine in allopurinol pharmaceuticals using zone fluidics and on-line solid phase extraction, J. Pharm. Biomed. Anal. 177 (2020), 112887.
[4] T. McGovern, D. Jacobson-Kram, Regulation of genotoxic and carcinogenic impurities in drug substances and products, Trac. Trends Anal. Chem. 25 (2006) 790–795.
[5] A.V. Reddy, J. Jaafar, K. Umar, et al., Identification, control strategies, and analytical approaches for the determination of potential genotoxic impurities in pharmaceuticals: A comprehensive review, J. Sep. Sci. 38 (2015) 764–779.
[6] T.D. Ho, M.D. Joshi, M.A. Silver, et al., Selective extraction of genotoxic impurities and structurally alerting compounds using polymeric ionic liquid sorbent coatings in solid-phase microextraction: Alkyl halides and aromatics, J. Chromatogr. A 1240 (2012) 29–44.
[7] B. Al-Sabti, J. Harbali, Development and validation of an analytical method for quantitative determination of three potentially genotoxic impurities in vildagliptin drug material using HPLC-MS, J. Sep. Sci. 44 (2021) 2587–2595.

[8] L. Chen, W. Zhang, S. Hu, Determination of genotoxic epoxide at trace level in drug substance by direct injection GC/MS, J. Pharm. Biomed. Anal. 146 (2017) 103–108.
[9] X.-W. Liu, W.-P. Zhang, H.-Y. Huan, et al., Trace determination of mutagenic alkyl toluenesulfonate impurities via derivatization headspace-GC/MS in an active pharmaceutical ingredient of a candidate drug, J. Pharm. Biomed. Anal. 155 (2018) 104–108.
[10] N. Scherer, K. Marcseková, T. Posset, et al., Evaluation of stir-bar sorptive extraction coupled with thermal desorption GC-MS for the detection of leachables from polymer single use systems to drugs, J. Pharm. Biomed. Anal. 152 (2018) 66–73.
[11] M. Lashgari, V. Singh, J. Pawliszyn, A critical review on regulatory sample preparation methods: Validating solid-phase microextraction techniques, Trends Anal. Chem. 119 (2019), 115618.
[12] S. Liu, Y. Huang, C. Qian, et al., Physical assistive technologies of solid-phase microextraction: Recent trends and future perspectives, Trends Anal. Chem. 128 (2020), 115916.
[13] X. Chen, X. Wu, T. Luan, et al., Sample preparation and instrumental methods for illicit drugs in environmental and biological samples: A review, J. Chromatogr. A 1640 (2021), 461961.
[14] N.B. Turan, S. Bakirdere, A miniaturized spray-assisted fine-droplet-formation-based liquid-phase microextraction method for the simultaneous determination of fenpiclonil, nitrofen and fenoxaprop-ethyl as pesticides in soil samples, Rapid Commun. Mass Spectrom. 35 (2021), e8943.
[15] B. Bojiko, N. Looby, M. Olkowicz, et al., Solid phase microextraction chemical biopsy tool for monitoring of doxorubicin residue during *in vivo* lung chemo-perfusion, J. Pharm. Anal. 11 (2021) 37–47.
[16] M. Sajid, J. Płotka-Wasylka, Combined extraction and microextraction techniques: Recent trends and future perspectives, Trends Anal. Chem. 103 (2018) 74–86.
[17] K.D. Clark, C. Zhang, J.L. Anderson, Sample preparation for bioanalytical and pharmaceutical analysis, Anal. Chem. 88 (2016) 11262–11270.
[18] Z. Feng, C. Huang, Y. Guo, et al., Graphitic carbon nitride derivative with large mesopores as sorbent for solid-phase microextraction of polycyclic aromatic hydrocarbons, Talanta 209 (2020), 120541.
[19] H. Piri-Moghadam, M.N. Alam, J. Pawliszyn, Review of geometries and coating materials in solid phase microextraction: Opportunities, limitations, and future perspectives, Anal. Chim. Acta 984 (2017) 42–65.
[20] L. Li, Y. Chen, L. Yang, et al., Recent advances in applications of metal-organic frameworks for sample preparation in pharmaceutical analysis, Coord. Chem. Rev. 411 (2020), 213235.
[21] I. Mohiuddin, A. Grover, J.S. Aulakh, et al., Porous molecularly-imprinted polymer for detecting diclofenac in aqueous pharmaceutical compounds, Chem. Eng. J. 382 (2020), 123002.
[22] J. Wang, J. Li, M. Gao, et al., Recent advances in covalent organic frameworks for separation and analysis of complex samples, Trends Anal. Chem. 108 (2018) 98–109.
[23] M. Huang, Z. Wang, J. Jin, Two-dimensional microporous material-based mixed matrix membranes for gas separation, Chem. Asian J. 15 (2020) 2303–2315.
[24] J. Chen, Y. Huang, X. Wei, et al., Covalent organic nanospheres: Facile preparation and application in high-resolution gas chromatographic separation, Chem. Commun. 55 (2019) 10908–10911.
[25] J. Staudinger, P.V. Roberts, A critical compilation of Henry's law constant temperature dependence relations for organic compounds in dilute aqueous solutions, Chemosphere 44 (2001) 561–576.
[26] J. Li, A.J. Dallas, D.I. Eikens, et al., Measurement of large infinite dilution activity coefficients of nonelectrolytes in water by inert gas stripping and gas chromatography, Anal. Chem. 65 (1993) 3212–3218.
[27] P. Fogg, J. Sangster, Chemicals in the Atmosphere: Solubility, Sources and Reactivity. John Wiley & Sons, Inc., 2003.
[28] S. Sarraute, H. Delepine, M.F. Costa Gomes, et al., Aqueous solubility, Henry's law constants and air/water partition coefficients of *n*-octane and two halogenated octanes, Chemosphere 57 (2004) 1543–1551.
[29] S. Sarraute, I. Mokbel, M.F. Costa Gomes, et al., Vapour pressures, aqueous solubility, Henry's law constants and air/water partition coefficients of 1,8-dichlorooctane and 1,8-dibromooctane, Chemosphere 64 (2006) 1829–1836.
[30] S. Karak, S. Kandambeth, B.P. Biswal, et al., Constructing ultraporous covalent organic frameworks in seconds via an organic terracotta process, J. Am. Chem. Soc. 139 (2017) 1856–1862.
[31] J. Li, H. Li, Y. Zhao, et al., A hollow microporous organic network as a fiber coating for solid-phase microextraction of short-chain chlorinated hydrocarbons, Mikrochim. Acta 185 (2018), 416.
[32] P. Rocío-Bautista, I. Pacheco-Fernández, J. Pasán, et al., Are metal-organic frameworks able to provide a new generation of solid-phase microextraction coatings? – A review, Anal. Chim. Acta 939 (2016) 26–41.
[33] J.M. Muñoz-Redondo, M.J. Ruiz-Moreno, B. Puertas, et al., Multivariate optimization of headspace solid-phase microextraction coupled to gas chromatography-mass spectrometry for the analysis of terpenoids in sparkling wines, Talanta 208 (2020), 120483.
[34] G. Ouyang, D. Vuckovic, J. Pawliszyn, Nondestructive sampling of living systems using *in vivo* solid-phase microextraction, Chem. Rev. 111 (2011) 2784–2814.
[35] M. He, X. Ou, Y. Wang, et al., Porous organic frameworks-based (micro) extraction, J. Chromatogr. A 1609 (2020), 460477.
[36] Z. Liu, H. Fan, Y. Zhou, et al., Development and validation of a sensitive method for alkyl sulfonate genotoxic impurities determination in drug substances using gas chromatography coupled to triple quadrupole mass spectrometry, J. Pharm. Biomed. Anal. 168 (2019) 23–29.
[37] T.D. Ho, P.M. Yehl, N.P. Chetwyn, et al., Determination of trace level genotoxic impurities in small molecule drug substances using conventional headspace gas chromatography with contemporary ionic liquid diluents and electron capture detection, J. Chromatogr. A 1361 (2014) 217–228.
[38] J.C.F. Menéndez, M.L.F. Sánchez, J.E. Sánchez Uría, et al., Static headspace, solid-phase microextraction and headspace solid-phase microextraction for BTEX determination in aqueous samples by gas chromatography, Anal. Chim. Acta 415 (2000) 9–20.
[39] T. Esteves, R. Viveiros, J. Bandarra, et al., Molecularly imprinted polymer strategies for removal of a genotoxic impurity, 4-dimethylaminopyridine, from an active pharmaceutical ingredient post-reaction stream, Sep. Purif. Technol. 163 (2016) 206–214.
[40] G. Székely, J. Bandarra, W. Heggie, et al., Design, preparation and characterization of novel molecularly imprinted polymers for removal of potentially genotoxic 1,3-diisopropylurea from API solutions, Sep. Purif. Technol. 86 (2012) 190–198.